Aerosol Science & Technology

ISSN: 0278-6826 (Print) 1521-7388 (Online) Journal homepage: https://www.tandfonline.com/loi/uast20

Calculation of Leakage and Particle Loss in Filter Cassettes

Paul A. Baron & James S. Bennett

To cite this article: Paul A. Baron & James S. Bennett (2002) Calculation of Leakage and Particle Loss in Filter Cassettes, Aerosol Science & Technology, 36:5, 632-641, DOI: 10.1080/02786820252883865

To link to this article: https://doi.org/10.1080/02786820252883865

Aerosol Science and Technology 36: 632–641 (2002)

Published by Taylor and Francis
0278-6826/02/$12.00 + .00

Calculation of Leakage and Particle Loss in Filter Cassettes

Paul A. Baron and James S. Bennett
Centers for Disease Control and Prevention, National Institute for Occupational Safety and Health, Cincinnati, Ohio

Experimental evidence of aerosol bypass leakage around the filter in plastic filter cassettes prompted an investigation using computational fluid dynamics to explain particle penetration through the leak. Axi-symmetric models of a cassette with several leak dimensions were constructed. The models predicted that submicrometer particles penetrated the leak, but that larger particles impacted on the filter surface. Experimental data from another study clearly indicated that larger solid particles were being lost from the surface of the filter during sampling. When particle bounce was invoked as an explanation for this loss of sampled solid particles, the theoretical loss from the filter in cassettes with large leaks exhibited characteristics similar to the experimental data. For small leaks, the mass loss behavior appeared to be more complex.

INTRODUCTION

Aerosol penetration through leaks has been a concern in several situations. Leakage in radioactive containment systems can release radioactive materials into the environment (Clement 1995; Morton and Mitchell 1995). Leakage through the face-seal in respirators can result in excess exposure of individuals to toxic gases and aerosols (Chen et al. 1990). In a recent study, a specially selected aerosol was used to seal leaks in ventilation ducts (Carrié and Modera 1998). Each of these applications involved a somewhat different leak geometry and different concerns regarding the fate of the aerosol particles. Recent experimental evidence of filter bypass leakage in personal sampling cassettes prompted investigation of the flow characteristics of these cassettes.

Plastic filter cassettes that are assembled by press-fitting components together to hold a filter are used extensively for industrial hygiene aerosol sampling in the United States and elsewhere. Many thousands of samples are collected each year using these cassettes, and inaccuracy of these samples may compromise the health of workers exposed to hazardous aerosols. These cassettes are produced in several diameters and configurations, with 25 mm and 37 mm diameter cassettes being the most common. Figure 1 shows the cross section of a 25 mm cassette to show how the pieces of the cassette fit together. The figure shows the ring fitted to the base to operate as an open face sampler. The ring also can be replaced by the cap to operate the cassette as a closed face sampler. During compression of the cap or ring to the base, the peripheral seal is achieved first and then further compression seals the edge of the filter and backup (support) pad and holds them in place. When this compression is performed properly, all the airflow passes through the filter and aerosol particles are collected on the filter for analysis. If insufficient or uneven compression is used, the edge of the filter may not be sealed, forming a leakage path from the interior of the cassette past the edge of the filter (bypass leakage). The possibility of air and particle leakage in these cassettes has been posed in the literature (Schmidt and Rappaport 1983; Frazee and Tironi 1987; Van den Heever 1994; Van den Heever and Tiernan 1999), but little documentation of the extent of this leakage and particle loss has been published. A recent investigation used a particle count leak test to estimate the extent of leakage and to provide a technique for evaluating cassette integrity (Baron et al. 2002). Either an optical particle counter or a condensation particle counter was used to measure penetration of ambient (primarily submicrometer) aerosol through the cassette as an indicator of leakage around the filter.

The experimental study (Baron et al. 2002) also indicated that a significant number of larger particles sampled in leaking cassettes bounced off the filter surface and through the leak. Particle bounce appeared to occur much more for solid particles than for oil droplets. Numerous reports of particle bounce in the literature indicated that particles have an increasing tendency to bounce with increasing size and velocity and with increasing deviation from the normal (90°) approach to the impaction surface. The shape and physical properties of the particle and the roughness and other properties of the impaction surface are also important. There have been several attempts to develop a

Received 1 May 2001; accepted 10 August 2001.

Mention of company names or products does not constitute endorsement by the Centers for Disease Control and Prevention.

Address correspondence to Paul Baron, Division of Applied Research and Technology, National Institute for Occupational Safety and Health, MS R3 4676 Columbia Parkway, Cincinnati, OH 45226. E-mail: pbaron@cdc.gov

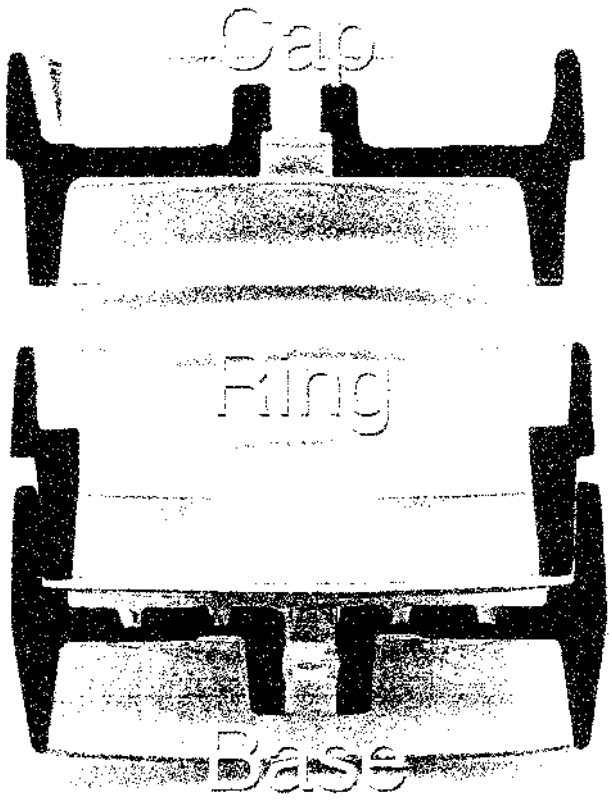

Figure 1. Picture of a 25 mm cassette cut in half with the cut cross section painted black for visibility. The filter is supported by a thicker cellulose backup (support) pad.

model of particle bounce (Xu and Willeke 1993; Dahneke 1995; Brach and Dunn 1998), but none of the theories apply to the situation presented in a leaking cassette, i.e., particles of unknown composition and shape impacting on the surface of various filter materials at acute angles.

To help explain the particle loss mechanisms for different types of particles, several axi-symmetric computational fluid dynamics (CFD) models of the same cassette configuration were developed. Each model assumed a uniform leak around the circumference of the filter, with only the height of the leak being varied. These models described the flow field in a leaking cassette and indicated the particle trajectories inside the cassette. The leak geometry in real cassettes is more complex than indicated in the models, but the CFD calculations permitted the evaluation of flow conditions and particle trajectories that were difficult to measure directly. Particle trajectories likely to result in particle bounce were evaluated for comparison to experimental data.

CFD MODELS

The flow field and particle trajectories within the cassette and filter were numerically modeled using CFD. The geometry was constructed and meshed using Gambit (Fluent Inc., Lebanon, NH), and the flow was solved using Fluent 5 (Fluent

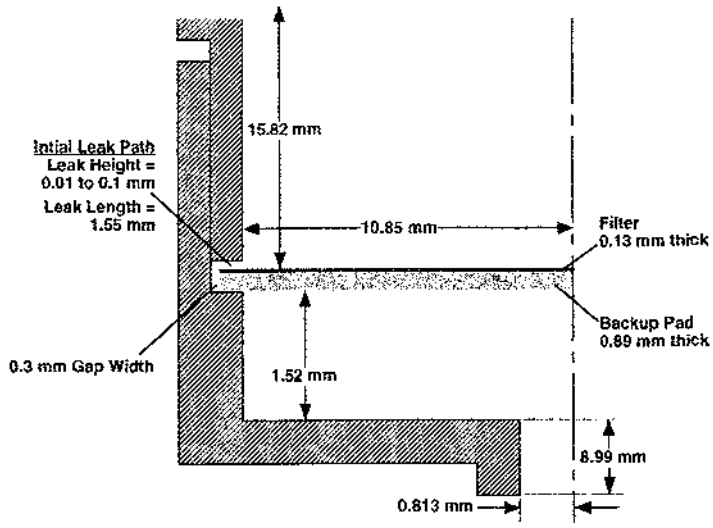

Figure 2. Schematic of half of a 25 mm filter cassette cross section. The dimensions indicated were used in the CFD model.

Inc., Lebanon, NH). To reduce the computational time for both mesh generation and flow solution, steady-state axi-symmetric simulations were performed. The dimensions of an idealized 25 mm open face cassette used in the models are shown in Figure 2. These dimensions were selected to be typical of those measured in several different examples of such cassettes. Nonuniform structured computational grids were generated using approximately 170,000 rectangular elements. Grid element density was increased in the area around the filter face and near and inside the leak to provide better resolution of the flow field and particle behavior. Grid element size at the cassette inlet was 4.5×10^{-9} m^2 and decreased monotonically toward the filter surface, where it was a minimum (1.6×10^{-11} m^2 for the largest leak and 5.4×10^{-12} m^2 for the smallest leak). The minimum element size also was used in a square area just upstream of the leak and inside the leak. Below the top filter surface, the elements were all 4.6×10^{-10} m^2. The walls, the inlet, and the outlet of the filter cassette formed the boundary conditions for the numerical solution. At the inlet, an ambient pressure boundary was specified. The flow rate (2.8 l/min) and the outlet area were used to specify the outlet velocity. The filter and filter backup pad were modeled as porous media using Darcy's Law. The material permeability was calculated from the pressure drop across the filter at a known velocity based on the manufacturer's specifications, with a pressure drop across the filter of 69000 N/m2 @ 0.33 m/s (10 psi @ 20 l/min/cm^2) and across the backup pad of 1700 N/m^2 @ 0.33 m/s (0.24 psi @ 20 l/min/cm^2). The initial leak path was modeled as a slot in the cassette wall with a rectangular cross section (Figure 2) between the top of the filter and the cassette ring flange, with the leak heights indicated in Table 1. The leak heights were chosen to span the range of the experimental results, with more leak heights in the small leakage range since more rapid changes in the leakage mechanisms appeared to be occurring in this range.

Table 1
Calculation results indicating the percent leakage through the CFD models with different leak heights; the 0.01 μm particle loss refers to particles entering the initial leak but not exiting it; the impaction diameters (d_{ae}) were calculated using the average velocity at the inlet and the exit to the initial leak.

Leak height (mm)	Air leak rate (%)	Loss of 0.01 μm particles (%)	d_{ae} (inlet) (μm)	d_{ae} (exit) (μm)
0.01	<0.47*		0.4	1.9**
0.02	1.4	38	0.5	0.6
0.025	3.3	19	0.5	0.6
0.03	6.0	8.5	0.6	0.6
0.05	37	4.8	0.7	0.8
0.1	75	3.1	1.4	1.6

*No streamline passed all the way through the smallest leak due to the limited spatial resolution of the model, so the air penetration value is presented as less than that if only one streamline passed through the leak.

**All streamlines in the leak entered the filter prior to reaching the exit of the initial leak. The air velocity at the end of the last streamline before it entered the filter was used to estimate the upper bound of the impaction diameter.

The flow rate and the dimensions of the cassette chamber and leak suggested that the flow was laminar, with Re <160. The outlet tube flow had Re of approximately 2,400. The range of Re, small leak size, and fine grid suggested that a 2 layer zonal model was indicated because the grid was fine enough to resolve the viscous sublayer near walls, including inside the leak. However, in the outlet tube and at locations where the flow could separate, as at the leak entrance, a higher Re model was suggested. The 2 layer zonal model could handle both flow domains, whereas many models use standard wall functions, which assume that the first cell adjacent to a wall is in the log-law region, causing the turbulent diffusivity to be overestimated. Some explorations using these standard wall functions resulted in lower velocity in and near the leak, since the inflated diffusivity gave the low velocity in the chamber more influence in the leak. As it turned out, though, the higher Re portion of the 2 layer zonal model was unnecessary, because in test cases spanning the range of leak sizes, the 2 layer zonal RNG k–ε turbulence model with residuals of 10^{-6} and the laminar case with residuals of 10^{-5} and 10^{-6} gave nearly identical results. Thus the proper turbulence model eventually converged to laminar flow in the important regions. Moreover, the turbulence model had shown that the largest turbulent Re occurred at the entrance to the cassette outlet tube, well downstream of the leak with its effect further dampened by the large flow resistance of the filter and backup pad. For solution economy, we relied on the laminar flow case, with residuals of 10^{-5}. Another way to evaluate convergence is to look at important variables as a function of iteration. We monitored wall shear stress inside the leak and pressure drop across the filter and found that these had become constant to 5 significant figures over several iterations when the residuals had reached 10^{-5}. Double precision (in the C computer language) was used to avoid problems with machine error.

In addition to solving the continuous phase, a discrete phase model was used to predict particle behavior using the Lagrangian particle tracking model available in Fluent 5. The discrete phase was represented as 427 spherical particles (1 kg/m^3 density) of a specified diameter injected at equal radial intervals at the inlet. The particle trajectories were calculated based solely on the flow field streamlines and only the effect of particle inertia was included. Particle interception (due to physical diameter of particle), gravitational settling, and diffusion were ignored. Particle diffusion was addressed in a separate model as indicated below. Particle-particle interactions and effects of the particles on the gas phase were assumed to be negligible due to the low volume fraction of the discrete phase. For the discrete-phase model, all solid surfaces were specified as trapping, which meant that any particle contacting a surface was removed from the air stream. The bottom surface of the filter was specified as trapping rather than the upper surface so that particle trajectories near the top surface could be visually tracked more easily. It was expected that particles would actually be collected at or near the top surface of the filter.

The models converged after 391–497 iterations (depending on leak height) so that the normalized residuals were below 10^{-3}. To test grid independence, the models were repeated with smaller and more numerous cells in regions of greatest wall shear stress gradient, such as near and in the leaks. Approximately 10,000 cells were added. The 2 sets of solutions agreed to within 1% on average based on air leak rate and 0.3 μm particle penetration. The finer grids were then used to generate the results reported here.

The leak height was quite small in some cases; so the effect of particle diffusion on deposition at various surfaces was considered. The primary area of interest was the area termed the initial leak path (Figure 2), i.e., between the filter edge and the cassette ring. The model flow fields were calculated only using laminar flow in the cassette, since the particle diffusion calculation module of Fluent did not operate with turbulence models. The laminar flow calculations were carried out with and without the diffusion feature turned on for comparison, since the number of trajectories penetrating the leak did not exactly match for the nondiffusion turbulence model and the diffusion laminar model.

RESULTS

Flow fields and particle trajectories were calculated for the scenarios indicated above. Particles with diameters of 0.3 μm, 0.8 μm, 2 μm, 3 μm, and 5 μm were injected uniformly into the inlet of the model. Example flow fields and 5 μm particle trajectories are displayed in Figures 3–5. The particles less than approximately 1 μm closely followed the airflow streamlines. However, larger particles did not easily make the 90° bend into

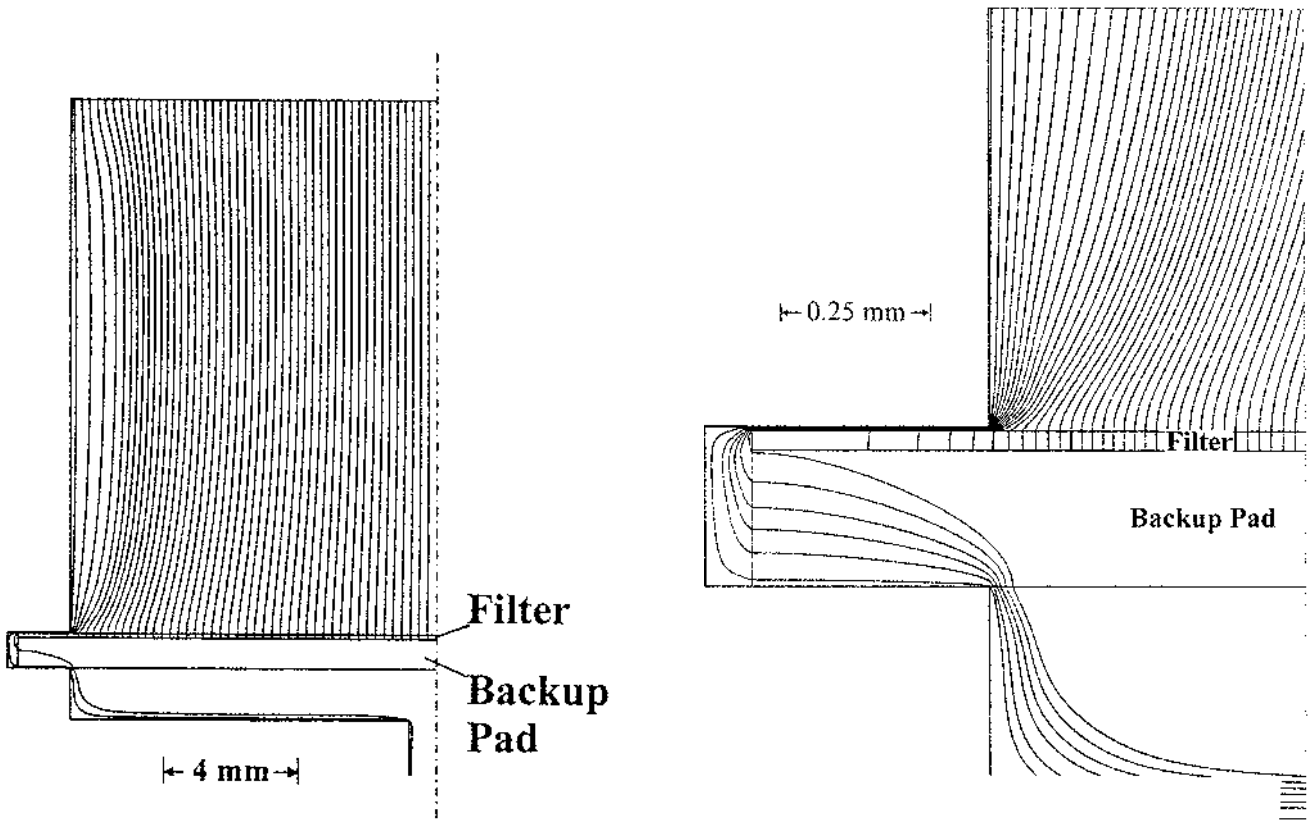

Figure 3. (a) Air streamlines in cassette with leak size 0.02 mm, resulting in 1.4% calculated air leakage past the filter. (b) Expanded view showing flow streamlines penetrating the leak and passing through the backup pad. Streamlines passing through the filter are stopped at the bottom surface of the filter to make it easier to track the leak streamlines.

the leak and were impacted on the filter surface near the leak entrance.

The leak heights in the CFD models were set at several levels. At each level, the percent leak rate was calculated using the number of streamlines or particle trajectories penetrating the leak (S) and the total number of streamlines or particle trajectories (427). To account for the cross-sectional area represented by each streamline or particle trajectory, the percent leak rate was determined using

$$\%\ \text{leak} = \frac{(427^2 - (427 - S)^2)}{427^2}. \qquad [1]$$

The results for percent air penetration through the leak are indicated in Table 1. The smallest-height leak model had no streamlines passing through the leak, so the penetration was presented as being less than that for 1 streamline passing through the leak. The results of the particle trajectory calculations of percent penetration for air, 6 particle diameters, and 5 leak heights are presented in Figure 6.

The effect of diffusion in the initial leak was calculated using only the laminar flow models. The penetration of particle trajectories through the initial leak path with and without diffusion turned on in the model gave nearly identical results.

The high velocity airflow between the filter and cassette should produce a normal lift force on the filter surface, effectively pulling the filter away from the backup pad and closing the leak. Because the upstream surface of the filter was modeled as a change in porosity rather than a true surface, the CFD models did not provide an indication of such a force. However, the models indicated that there was an equivalent normal force on the cassette wall. This suggested that there was such a force on the filter surface.

In the experimental study of cassette leakage, a test was developed that used ambient submicrometer particles as an indicator of bypass leakage (Baron et al. 2002). These test results were compared with mass lost from the filter while sampling an aluminum oxide aerosol with a count median diameter of 3.6 μm. The comparison of submicrometer particle leakage and mass lost from the filter produced an unexpected nonlinear relationship between these 2 parameters (Figure 7). This experimental comparison was simulated using the CFD calculations, with 0.3 μm particles representing the ambient aerosol penetrating the leak (as an indicator of leak size) and 5 μm particles

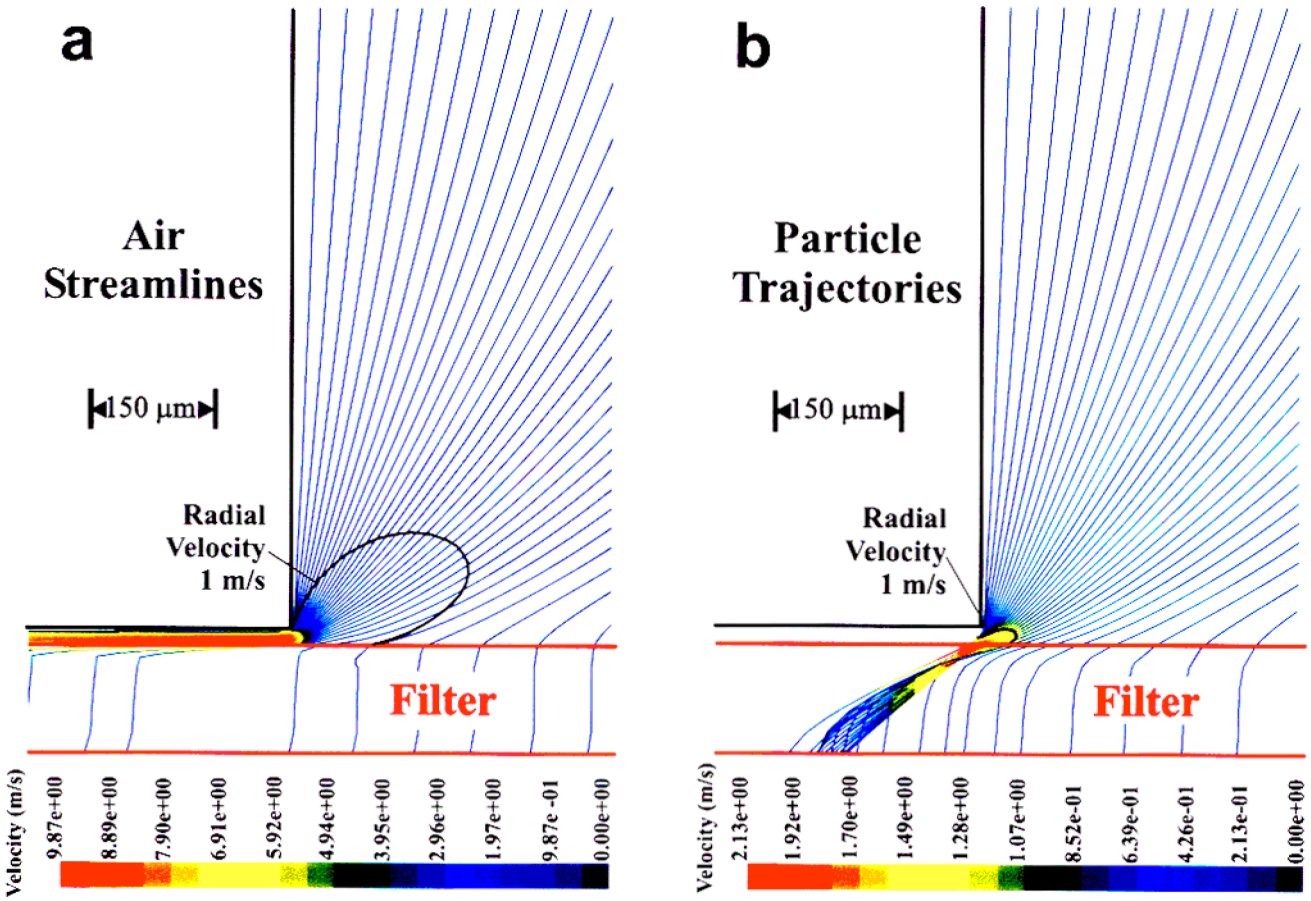

Figure 4. (a) A further expansion of Figure 3 in the neighborhood of the leak. Not all calculated streamlines are shown. Radial air velocities are indicated in color. (b) 5 μm particle trajectories in the vicinity of the leak in the same expanded view. The region where the radial velocity of the particles was >0.5 m/s is indicated by the contour line. Particles passing through the filter are also stopped at the bottom surface of the filter to make it easier to track the particle trajectories. Particle radial velocities are indicated by color.

representing the aluminum oxide aerosol at the corresponding leak sizes. To estimate the mass lost from the filter, trajectories of 5 μm particles having a radial velocity >0.5 m/s were selected as representing particles likely to bounce from the filter surface. This selection criterion was chosen to indicate particles approaching the surface at a high velocity and an acute angle. The results are plotted in Figure 7 along with data from the experimental study (Baron et al. 2002). Similar calculations of particle bounce were made using radial velocities of 0.5 m/s and 0.25 m/s as selection criteria. The loss due to bounce at the smallest leak size increased from 0 to 7.4%, while the loss at larger leak sizes increased only about 5%.

The total flow rate through the cassette was varied to see the effect on the relative flow through the leak versus the filter. The model with a leak height of 0.03 mm was calculated at a flow rate of 15 l/min. The percent flow through the leak at 2.8 l/min was calculated to be 6.0% versus 8.3% at the higher flow rate. Thus as the flow rate through the cassette increased by more than a factor of 5, the fraction of air passing through the leak rather than the filter increased only by a factor of 1.38.

DISCUSSION

The CFD models used in this study were axi-symmetric models that assumed a uniform leak height and cross section around the edge of the filter. The actual leak geometries were likely to be considerably more complex, with variation from one side of the cassette to the other and smaller local variations in leak cross sections. Thus the models only represented the average leak geometry for a given total leak rate.

The models converged and appeared physically reasonable. The example flow field shown in Figure 3 indicates several features of relevance to the collection and loss mechanisms. The divergence of the streamlines at the outer wall of the cassette was a result of the developing boundary layer (Figure 3a). Across the collection surface of a well-sealed cassette, the

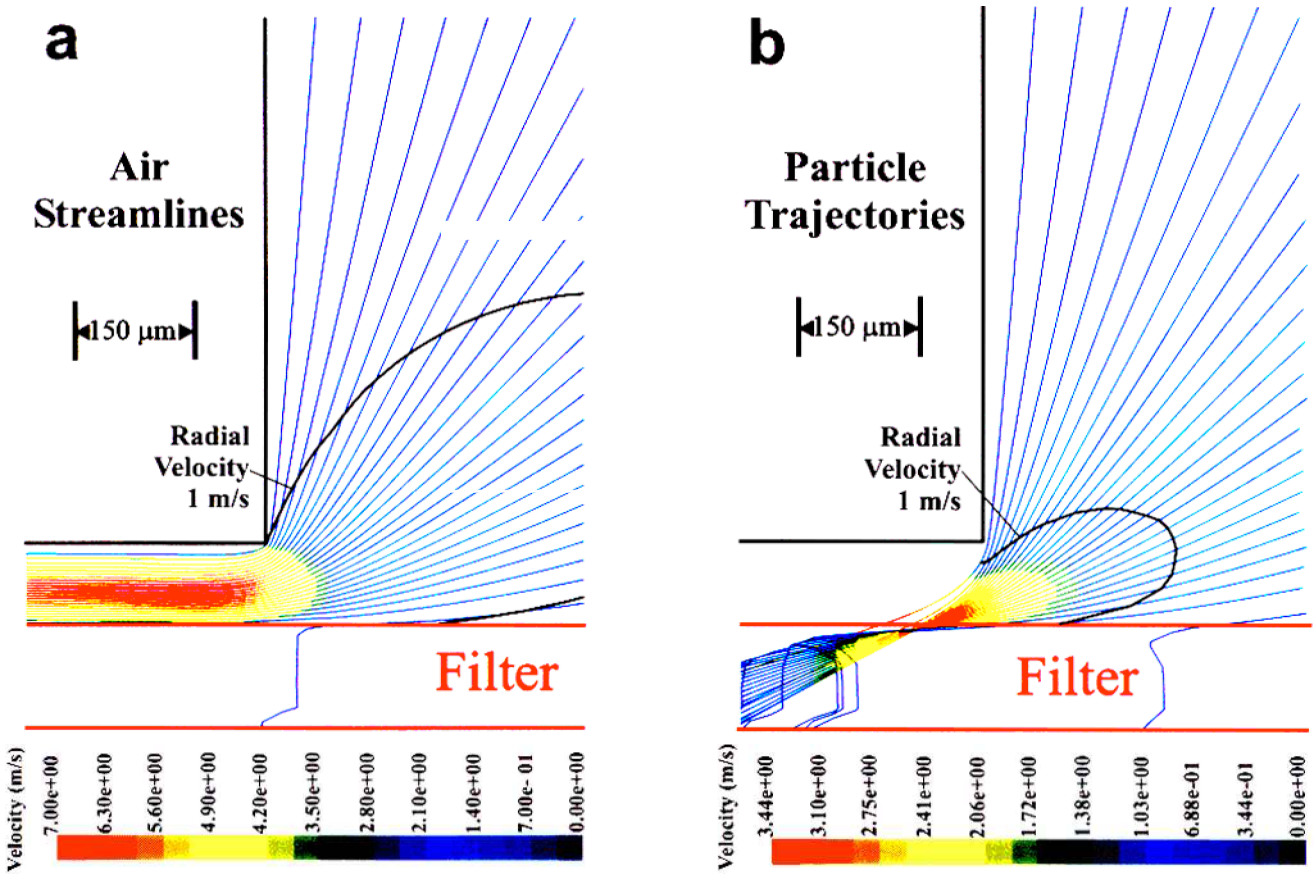

Figure 5. (a) Air streamlines in a cassette with leak size 0.1 mm, resulting in 76% calculated air leakage past the filter. The magnification is the same as in Figure 4a. (b) 5 μm particle trajectories in the vicinity of the leak in the same expanded view.

filter had a uniform pressure drop, forcing the streamlines to be uniformly spaced similarly to the inlet condition and the particles deposited on the filter uniformly. With a leaking cassette, some streamlines were focused toward the filter near the entrance to the leak (Figures 4a and 5a). The air motion toward the leak produced focusing of larger particles toward the filter surface in the proximity of the leak (Figures 4b and 5b). Most of the air entering the leak made a sharp bend prior to the leak. This bend caused impaction of larger particles onto the filter surface. The models predicted that particles smaller than about 1–2 μm passed into the leak without depositing on the filter, while larger particles impacted the filter surface (Figure 6).

For the smallest leak size, several streamlines entered the leak, but most passed through the edge of the filter so that no streamlines exited the leak. Submicrometer particles followed these streamlines so that air entering the leak still accelerated particles toward the leak, but the particles were less likely to penetrate the leak entirely, with a fraction of the particles depositing on the edge of the filter. Thus submicrometer particles measured downstream of the filter were still an indication of the airflow entirely bypassing the filter, but the behavior of larger particles was likely to be more complex. The smallest leak modeled here had a height of only about 10 μm. Thus large particles bouncing from the filter surface had a limited probability of entering and penetrating the leak. The calculation resulting in the curve in Figure 7 was performed assuming that particles with high radial velocity would bounce and penetrate the leak. With such a small leak opening, the particles could hit the walls of the cassette both inside and outside the leak and eventually end up on the filter.

The simple bounce model does not explain the shape of the experimental data in Figure 7 for small leaks, but still appears reasonable for larger leaks. It is clear that for 0 leakage, the submicrometer particles penetrating the cassette and large particle loss from the filter are both 0. For very small leaks, air streamlines enter the leak, but most of the streamlines pass through the filter edge. As the leak size increases, the fraction of air entering the leak and bypassing the filter increases rapidly, so that at some point most of the air entering the leak bypasses the filter. Submicrometer particles closely follow the air streamlines. The collection of submicrometer particles on the edge of the filter explains the general shape of the experimental data, effectively shifting the curve such that for large leaks, the slope is constant

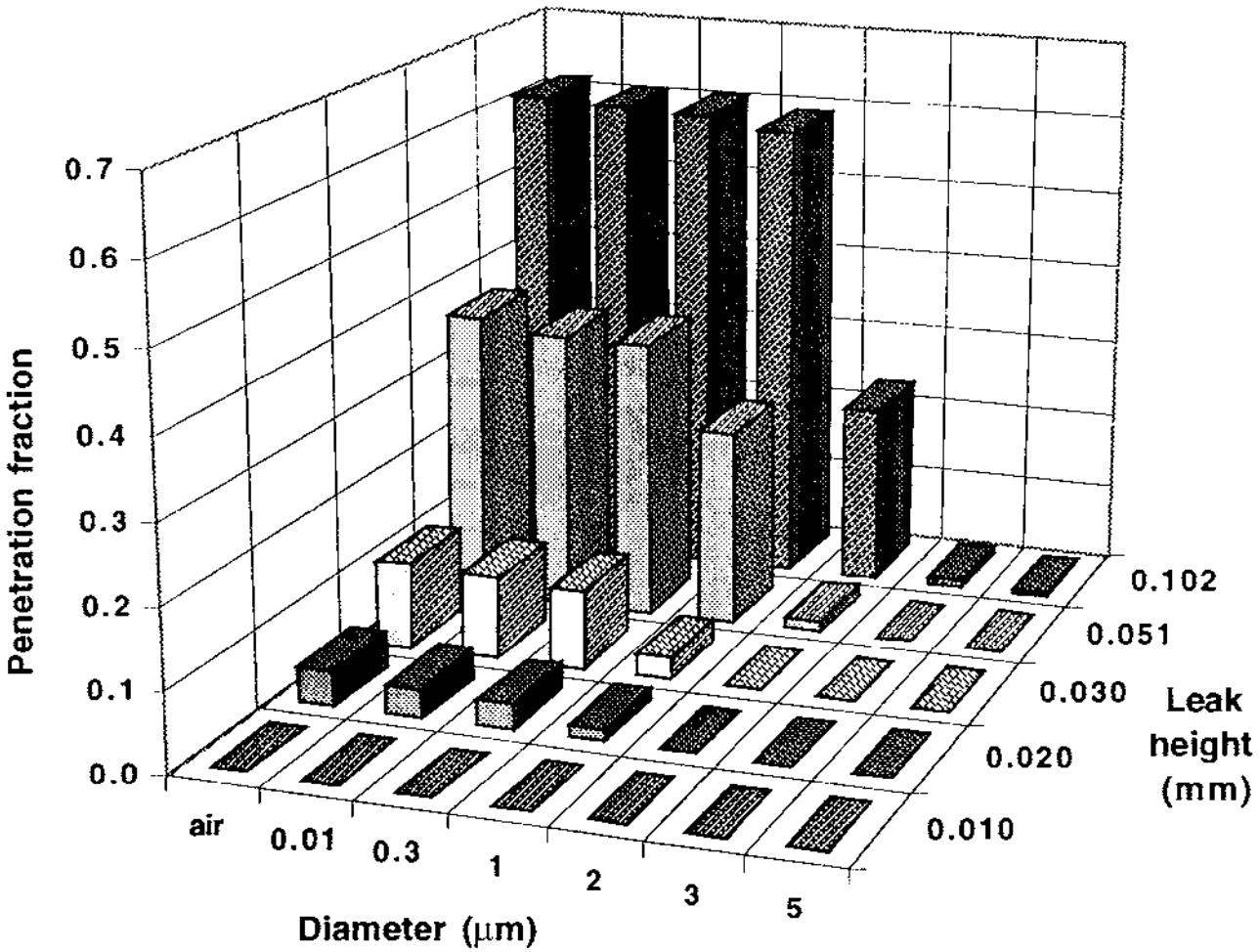

Figure 6. Calculated penetration of air and particles through several leaks with different sizes. Note that the x and y scales are not linear.

and near unity but with a nonzero intercept. The large particle mass loss for small leaks is difficult to model exactly because of the small size of the leak opening. Particles that initially bounce off the filter surface may subsequently bounce off other surfaces and eventually be deposited either on the filter edge, the cassette wall, or on the filter collection surface. The experimental data indicates that up to a measured small particle penetration of about 4%, the large particle penetration increases with a slope of about 4, and then quickly levels out to a slope close to unity. This transition corresponds in the simulations to the change from streamlines entering the leak but passing through the filter edge to streamlines entering the leak and largely bypassing the filter.

Particle diffusion appears likely to result in only minor losses of countable particles in the leak channel between the filter and cassette. Inexpensive particle counters that can be used for measuring ambient aerosol leakage in cassettes, such as a condensation particle counter or optical particle counter, have lower particle size detection limits of about 0.02 and 0.3 μm, respectively. The calculated loss of 0.01 μm particles (Table 1) represents a very conservative upper bound on the losses of larger particles detectable by these instruments. Thus measurement of submicrometer particles downstream of the cassettes will indicate the presence of a leak, assuming that these particles are not lost in the backup pad and that the filter is 100% efficient for all particles.

The models should predict reasonably well the relative amount of airflow through the leak versus the filter and the behavior of aerosol particles approaching, entering, and passing through the initial leak path. The fraction of airflow through the leak changes rapidly with leak height, increasing more than 2 orders of magnitude for 1 order of magnitude increase in leak height. The calculation of the flow rate dependence of the flow ratio between the leak and the filter indicates that the ratio does not change greatly. Thus the particle count leak test should not depend significantly on the test flow rate as long as the high flow rate does not significantly distort the leak size and geometry.

Downstream of the initial leak path, the flow was calculated to pass through the backup pad, modeled as a uniform flow

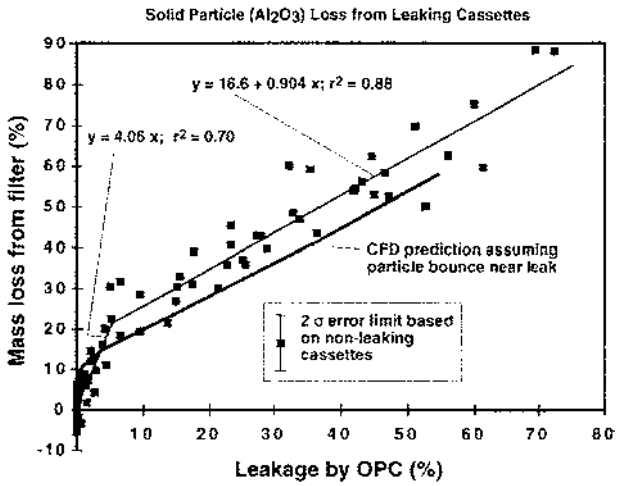

Figure 7. Comparison of data on loss of mass of aluminum oxide dust versus particle count leak test measurements of submicrometer ambient air (Baron et al. 2002) with CFD calculations under similar conditions.

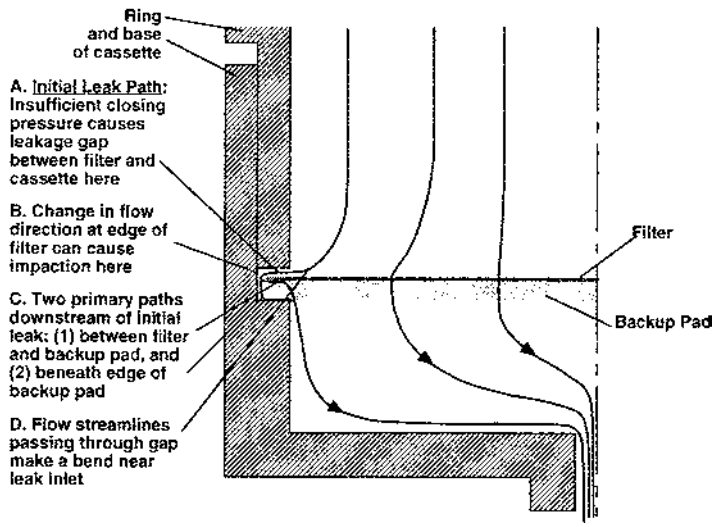

Figure 8. Schematic cross section of half of the filter cassette with example flow streamlines (from Baron et al. (2002)). An increasing gap height causes an increasing fraction of air to pass through the leak versus through the filter. The filter is porous, but particle retentive; the backup pad is even more porous and assumed to be nonparticle retentive. The observed path through the backup pad appears more complex than that used in the models.

resistance, filling completely the region below the filter edge. This assumption appeared not to agree with the path taken by particles as observed through deposition patterns of submicrometer soot particles (Baron et al. 2002). Two primary paths appeared to be (1) between the filter and backup pad near the edge of the filter and then down through the backup pad, and (2) between the bottom edge of the backup pad and the cassette base sealing surface (Figure 8). The high velocity airflow through the initial path of the leak suggests there was an upward force pulling the filter away from the backup pad. This would enhance the likelihood of the first leak path. The complex path taken by the aerosol was difficult to model as it depended on details of the shape and deformation of both the filter and backup pad under leak conditions. The assumption that particles passed through the backup pad with no loss was also clearly incorrect, but the main focus of the CFD calculations was the loss of particles that should have been collected on the filter surface. The loss of particles once the aerosol particles bypassed the filter surface was only of interest to determine the detection efficiency of the particle counter used for the leak test. The CFD calculations could not provide details on this latter aspect of cassette leakage.

Inside the leak, the streamlines are compressed, indicating a relatively high velocity region (typically on the order of 5 m/s at the leak inlet), and make a sharp bend past the outer edge of the filter and then down through the backup pad (see Figures 3b and 8). Note that the air velocity increases until the streamline compression reaches a maximum inside the initial leak, then decreases as the air passes through the initial leak, as is especially evident in Figure 4a. The decreasing velocity in the leak is due to airflow down through the filter, to an increase in cross-sectional area of the leak as the radial distance from the center of the cassette increases, and to streamline expansion as the flow passes through the leak. The outer cassette wall near the edge of the filter, as indicated in Figure 8b, is a likely location for impaction of larger particles that might have entered the leak. The Stokes number (Stk) characterizes particle inertial behavior and is the ratio of the particle stopping distance to the characteristic dimension of the air stream. In this context

$$\mathrm{Stk} = \rho_p {d_{ae}}^2 VC_c/9\eta d_j, \qquad [2]$$

where ρ_p is the particle density, d_{ae} is the particle aerodynamic diameter, V is the average air velocity at the leak entrance, C_c is the slip correction factor, η is the air viscosity, and d_j is the inlet size (leak height). Considering the exit region of the leak slot as an impactor with a rectangular jet, particles with $\sqrt{(\mathrm{Stk})} > 0.84$ are likely to impact. The $\sqrt{(\mathrm{Stk})}$ for impaction on the cassette wall was calculated using average air velocity at the edge of the filter. The results indicated that particles greater than about $d_{ae} = 0.6 - 1.9$ μm aerodynamic diameter passing through the leak were likely to impact on the wall of the cassette (Table 1). The Stokes number may also be used to estimate the likelihood of losses in inlets (Brockmann 1993). A similar calculation was made for the inlet of the leak (Table 1) to indicate those particles likely to impact onto the filter. Thus submicrometer particles can penetrate the entire cassette, while larger particles can penetrate only after they have bounced, probably more than once, within the cassette. Although deposits were observed in the expected impaction region on the outer cassette wall near the edge of the filter, there was also a significant amount of penetration of larger

solid particles through the entire cassette in the experimental study of leakage (Baron et al. 2002), indicating particle bounce here as well.

The CFD program is not capable of estimating the degree of particle bounce because this involves complex interactions between particles impacting either the filter surface or particles previously collected. Experimental and theoretical work by several researchers indicates that particles are more likely to bounce when they have high kinetic energy, have acute approach angles ($\ll 90^\circ$), are solid (versus liquid) particles, and impact on smooth (versus rough) surfaces (John and Sethi 1993; Xu and Willike 1993; Xu et al. 1993; Brach and Dunn 1998; Li et al. 1999, 2000). The air and particle velocity in a nonleaking cassette was about 0.13 m/s normal to the filter surface, while particle velocities near a leak could exceed 5 m/s with a large radial velocity component. A large radial velocity of the particles at impact provided an indication of particles having a high kinetic energy and a trajectory with an acute angle to the filter surface. In addition, any particles that bounced were likely to be swept into the leak by the high velocity stream parallel to the filter surface in and near the leak. The filter surface was not smooth, but the high kinetic energy combined with an acute angle of approach suggested a high likelihood of bounce. A radial velocity component of 0.5 m/s was arbitrarily chosen as the cutoff value for particles likely to bounce. Although this cutoff was arbitrary, the high particle acceleration near the leak inlet meant that the number of trajectories chosen to represent the area from which particles bounced using this cutoff was not very sensitive to the absolute value of the velocity cutoff. As indicated in Figure 7, using the 0.5 m/s cutoff provided filter mass loss values that matched the observed aluminum oxide dust loss data as a function of submicrometer particle penetration reasonably well (Baron et al. 2002). At small leak rates, the rapid increase in particle loss with increasing leak rate is due to the relatively large area from which particles are attracted to the leak. Above a leak size of several percent, the area increases with percent leakage in a nearly one-to-one relationship.

Considering the number of assumptions that went into construction of the CFD models, the close agreement with the experiment was remarkable, but may have been fortuitous. In addition to the selection of radial velocity as an indicator of particle bounce, the horizontal axis in Figure 7 did not depend solely on airflow through the leak. In the experiments, the fraction of submicrometer particles passing through the initial leak but collected in the backup pad may have varied with percent leakage, aerosol loading in the cassette, and particle type. Some combination of these undetermined factors may have contributed to the close agreement between the CFD model and the experimental data. However, the shape of the data curve in Figure 7 was initially unexpected, with a sharp break in the mass loss curve at around 4% penetration of submicrometer particles. The fact that the slope, and to some extent the shape, of the CFD-derived curve agreed with the experimental data supports the likelihood of particle bounce being the primary loss mechanism for solid dust particles sampled using leaking cassettes.

SUMMARY

In a sampling cassette, incomplete compression of the seal holding the filter and backup pad can result in a leak around the edge of the filter. The predicted fraction of air passing through the leak increases rapidly with increasing leak height, reaching 75% for 0.1 mm leak height. Particles smaller than about 0.6–1.9 μm can follow the air streamlines and pass through the leak, around the filter, through or around the backup pad, and out of the cassette. In most modern personal samplers, the filter is sufficiently efficient that >99.9% of all particles that pass through the filter are collected. The calculations indicate that submicrometer particles penetrate the leak with the same efficiency as the air, although this does not take into account particle losses in the backup pad. Thus submicrometer particles are likely to be a useful indicator of bypass leakage in cassettes using high efficiency filters. The calculations further suggest that large particle (>about 2 μm) penetration through the leak occurs only when the particles can bounce from the filter surface. Thus large particle loss from the filter will be a function of particle bounce characteristics, such as particle diameter distribution, physical state (e.g., solid or liquid), and filter properties.

REFERENCES

Baron, P. A., Khanina, A., Martinez, A. B., and Grinshpun, S. A. (2002). A Leak Test for Aerosol Sampling Cassettes, *Aerosol Sci. Technol.*, in press.

Brach, M., and Dunn, P. F. (1998). Models of Rebound and Capture for Oblique Microparticle Impacts, *Aerosol Sci. Technol.* 29:379–388.

Brockmann, J. (1993). Sampling and Transport of Aerosols. In *Aerosol Measurement: Principles, Techniques and Applications*, edited by K. Willeke and P. A. Baron. Van Nostrand Reinhold, New York, pp. 77–111.

Carrié, F. R., and Modera, M. P. (1998). Particle Deposition in a Two-Dimensional Slot from a Transverse Stream, *Aerosol Sci. Technol.* 28:235–246.

Chen, C. C., Ruuskanen, J., Pilacinski, W., and Willeke, K. (1990). Filter and Leak Penetration Characteristics of a Dust and Mist Filtering Facepiece, *Am. Ind. Hyg. Assoc. J.* 51:632–9.

Clement, C. F. (1995). Aerosol Penetration through Capillaries and Leaks: Theory, *J. Aerosol Sci.* 26:369–386.

Dahneke, B. (1995). Particle Bounce or Capture–Search for an Adequate Theory: I. Conservation-of-Energy Model for a Simple Collision Process, *Aerosol Sci. Technol.* 23:25–39.

Frazee, P. R., and Tironi, G. (1987). A Filter Cassette Assembly Method for Preventing Bypass Leakage, *Am. Ind. Hyg. Assoc. J.* 48:176–180.

John, W., and Sethi, V. (1993). Threshold for Resuspension by Particle Impaction, *Aerosol Sci. Technol.* 19:69–79.

Li, X., Dunn, P. F., and Brach, R. M. (1999). Experimental and Numerical Studies on the Normal Impact of Microspheres with Surfaces, *J. Aerosol Sci.* 30:439–449.

Li, X., Dunn, P. F., and Brach, R. M. (2000). Experimental and Numerical Studies of Microsphere Oblique Impact with Planar Surfaces, *J. Aerosol Sci.* 31:583–594.

Morton, D. A. V., and Mitchell, J. P. (1995). Aerosol Penetration through Capillaries and Leaks: Experimental Studies on the Influence of Pressure, *J. Aerosol Sci.* 26:353–368.

Schmidt, A. C., and Rappaport, S. M. (1983). *An Evaluation of Filter Bypass Leakage in 37 mm Plastic Filter Cassettes*, American Industrial Hygiene Association Conference, Philadelphia, PA.

Van den Heever, D. J. (1994). Quantification of Bypass Leakage in Two Different Filter Cassettes during Welding Fume Sampling, *Am. Ind. Hyg. Assoc. J.* 55:966–969.

Van den Heever, D. J., and Tiernan, G. (1999). Quantification of Bypass Leakage in Filter Holders with Cyclone Elutriators, *Am. Ind. Hyg. Assoc. J.* 60:545–547.

Xu, M., and Willeke, K. (1993). Right Angle Impaction and Rebound of Particles, *J. Aerosol Sci.* 24:19–30.

Xu, M., Willeke, K., Biswas, P., and Pratsinis, S. (1993). Impaction and Rebound of Particles at Acute Incident Angles, *Aerosol Sci. Technol.* 18:143–155.